

RESEARCH ARTICLE OPEN ACCESS

Molecular Subtypes and Immune Microenvironment Characterization of the Annulus Fibrosus in Intervertebral Disc Degeneration: Insights From Translation Factor-Related Gene Analysis

Sikuan Zheng^{1,2,3,4} | Xiaokun Zhao^{1,2,3,4} | Hui Wu^{1,2,3,4} | Xuhui Cuan¹ | Xigao Cheng^{1,2,3,4} | Dingwen He^{1,2,3,4} 

¹Department of Orthopedics, The Second Affiliated Hospital of Nanchang University, Nanchang, Jiangxi Province, China | ²Institute of Orthopedics of Jiangxi Province, Nanchang, Jiangxi Province, China | ³Institute of Minimally Invasive Orthopedics, Nanchang University, Nanchang, Jiangxi Province, China | ⁴Jiangxi Provincial Key Laboratory of Spine and Spinal Cord Disease, Nanchang, Jiangxi Province, China

Correspondence: Xigao Cheng (ndefy12160@ncu.edu.cn) | Dingwen He (hedingwen@126.com)

Received: 19 November 2024 | **Revised:** 5 March 2025 | **Accepted:** 24 March 2025

Funding: The authors received no specific funding for this work.

Keywords: annulus fibrosus | immune landscape | intervertebral disc degeneration | molecular subtype | translation factors

ABSTRACT

Objective: This study aims to examine the role of translation factors (TF) in intervertebral disc degeneration (IVDD) and to evaluate their clinical relevance through unsupervised clustering methods.

Methods: Gene expression data were retrieved from the GEO database, and the expression levels of translation factor-related genes (TFGs) were extracted for analysis.

Results: Two distinct molecular clusters were identified based on the differential expression of nine significantly altered TFGs. Immune infiltration was notably higher in Cluster C2 compared to Cluster C1. Subsequently, two gene clusters were identified based on the differentially expressed genes between the clusters. A Sankey diagram illustrated a high degree of consistency between the molecular clusters and the gene clusters. Additionally, four machine learning models were developed and evaluated, with the SVM model being utilized to construct a nomogram for predicting the incidence of IVDD. Validation using external datasets and clinical samples confirmed the low expression of EEF2K, which was further analyzed in a pan-cancer context.

Conclusion: The identification and comprehensive assessment of the two molecular clusters offer significant insights for the classification and treatment of individuals with IVDD.

1 | Introduction

Intervertebral disc degeneration (IVDD) is the primary contributing factor to low back pain (LBP) and is characterized by a complex pathogenesis [1]. The development of IVDD can result from various factors, including genetic predisposition, overweight or obesity, and unhealthy lifestyle choices. Currently, effective non-surgical interventions for reversing IVDD remain limited, largely due to an incomplete understanding of

its underlying mechanisms. A deeper comprehension of IVDD pathogenesis may offer opportunities to slow disease progression and reduce the prevalence of disability. Therefore, investigating IVDD subtypes, identifying key genes associated with the condition, and elucidating the underlying mechanisms may lead to the development of new therapeutic strategies.

A Study has shown that annulus fibrosus (AF) injury is closely related to disc degeneration [2]. The AF is a rigid annular part

This is an open access article under the terms of the [Creative Commons Attribution-NonCommercial-NoDerivs](https://creativecommons.org/licenses/by-nc-nd/4.0/) License, which permits use and distribution in any medium, provided the original work is properly cited, the use is non-commercial and no modifications or adaptations are made.

© 2025 The Author(s). JOR Spine published by Wiley Periodicals LLC on behalf of Orthopaedic Research Society.

that forms the outer layer of the intervertebral disc and is characterized by nonlinearity, anisotropy, and viscoelasticity. It wraps around the nucleus pulposus (NP), prevents herniation of the NP tissue, and maintains spinal stability and disc strength. A deeper understanding of the specific events affecting the AF and NP disc compartments may provide opportunities to explore disc disease progression and propose new therapeutic strategies. However, the subtypes of AF and the immune microenvironment remain unclear.

Huang et al. [3] found that neutrophil infiltration showed the highest significant correlation with central genes such as *ULK1* and *SQSTM1*, and that neutrophils and $\gamma\delta$ T cells were closely associated with the progression of IDD. Moreover, there were

significant differences in immune profiles between different IDD subtypes [4]. Translation factors (TF) play key roles in processes like cell growth, division, and apoptosis by facilitating the recruitment of ribosomes to mRNA and regulating the elongation of polypeptide chains [5–8]. While it is well established that TF abnormalities can lead to various diseases, particularly cancer, their impact on cellular function in higher organisms remains largely unexplored [9]. Recent research has only gradually begun to uncover the roles of TF in higher organisms. For instance, Eyries et al. identified four biallelic *EIF2AK4* mutations in sporadic cases of pulmonary veno-occlusive disease (PVOD), establishing *EIF2AK4* as a key gene implicated in the development of PVOD [10]. Xu et al. found that *EIF2AK4* is involved in Sesn2-mediated mitophagy involved in disc degeneration [11].

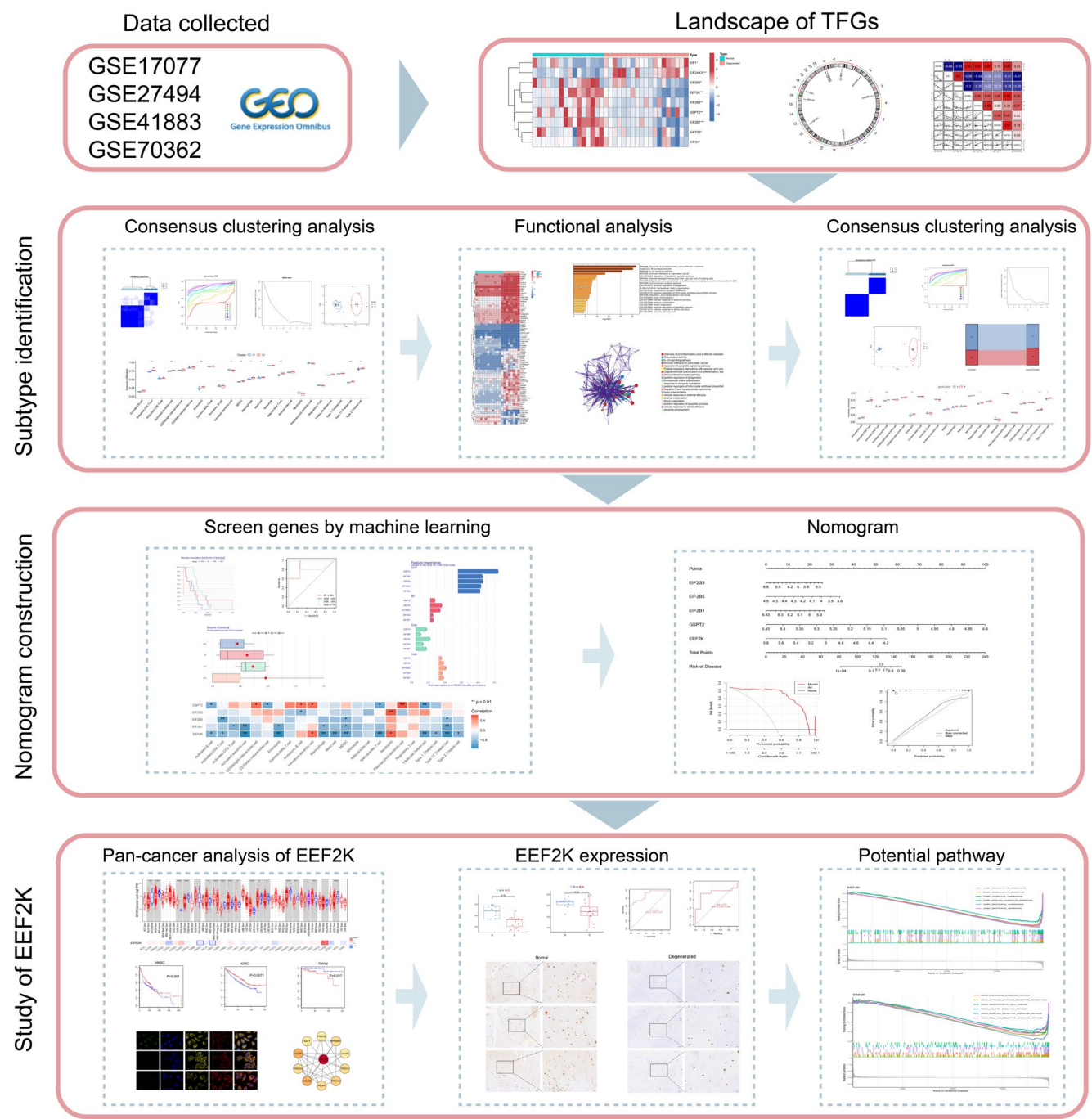


FIGURE 1 | Study flowchart: Overall study diagram.

Additionally, mutations in *eIF2B* have been directly linked to vanishing white matter disease (VWMD) and permanent neonatal diabetes mellitus (PNDM) [12]. Despite these advancements, the role of TF in IVDD remains unclear.

This study conducted a comprehensive assessment of the characterization and immune infiltration of two clusters using the GSE27494, GSE17077, GSE41833, and GSE70362 datasets. The GSE datasets were from AF samples, and that unsupervised clustering analysis identified differential changes in TG. Moreover, Immune cell infiltration was analyzed in different groups. The analysis revealed a high degree of consistency between the outcomes of the two clusters, which may influence the classification and treatment approaches for IVDD. Furthermore, a nomogram incorporating five TF-related genes (*EIF2S3*, *EIF2B5*, *EIF2B1*, *GSPT2*, and *EEF2K*) was developed, demonstrating accurate predictions of IVDD incidence. Additionally, the study validated the expression of *EEF2K* and examined its significance in a pan-cancer context. A schematic representation of the study is depicted in Figure 1.

2 | Materials and Methods

2.1 | Data Acquisition and Processing

The GEO database (<https://www.ncbi.nlm.nih.gov/geo/>) provided five distinct AF groups: GSE27494 ($n=8$), GSE17077 ($n=19$), GSE41833 ($n=8$), and GSE70362 ($n=24$) (Table S1).

The three GEO datasets (GSE27494, GSE17077, GSE41833) were merged, and the R package “SVA” was used to normalize the expression levels across different batches. The combined data served as the test set, while GSE70362 was designated as the validation set. Fifty TFGs were obtained from the GSEA “WP_TRANSLATION_FACTORS” pathway (<http://www.broadinstitute.org/gsea/>) (Table S2).

2.2 | TFG Landscape

Differential analysis of the 50 TFGs was conducted using the “limma” R package, with a significance threshold set at $p<0.05$. The chromosomal localization of TFGs was visualized using the R “circos” package. Heatmaps were used to display the expression levels of the differential TFGs across the samples.

2.3 | Consensus Cluster Analysis

Unsupervised consensus analysis was conducted on 19 patients diagnosed with IVDD using the “ConsensusClusterPlus” R package. The analysis involved 1000 resamples, each consisting of 80% of the samples. The optimal number of clusters (k) was determined using a Consensus Cumulative Distribution Function (CDF) plot. Finally, principal component analysis (PCA) was used to assess the clustering results.

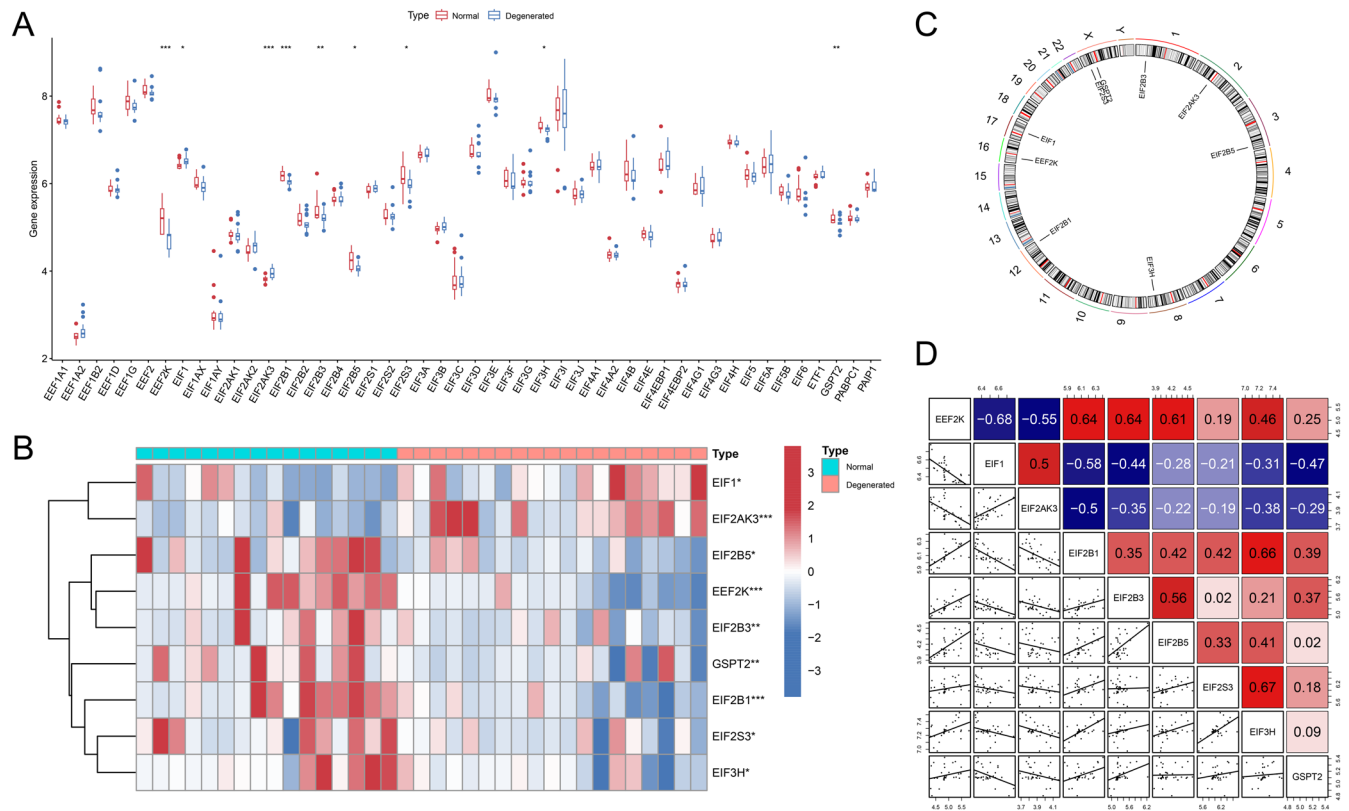


FIGURE 2 | Landscape of TFGs. (A) The differential expression boxplot of 50 TFGs. (B) Heatmap depicting nine significant TFGs. (C) Chromosome position. (D) Heatmap for correlation analysis.

2.4 | ssGSEA and GSEA

Immune cell infiltration was analyzed using single-sample gene set enrichment analysis (ssGSEA) with the “GSVA” R package. Subsequently, correlations between immune cells, clusters, and key genes were assessed. To further elucidate the potential roles of the biomarkers, GSEA was performed on specific genes using the “c2.cp.kegg.symbols.gmt” and “c5.go.symbols.gmt” datasets.

2.5 | Machine Learning Models

Based on the differentially expressed TFGs, four machine learning models (Random Forest, Support Vector Machine, Generalized Linear Model, and eXtreme Gradient Boosting) were developed using the “caret” package. The differentially expressed TFGs served as explanatory variables, with IVDD samples as the response variable. The performance of the four models was assessed using the “DALEX” package. Finally, the importance of the differentially expressed TFGs in predicting the response variable was assessed.

2.6 | Nomogram for IVDD

The nomogram was developed using the “rms” package to clinically predict the occurrence of IVDD. The calibration performance and clinical value of the model were assessed through the use of a calibration curve and decision curve analysis.

2.7 | Pan-Cancer Analysis

The online TIMER platform (<https://cistrome.shinyapps.io/timer/>) was used to assess the expression of EEF2K mRNA across various cancer types. The prognostic significance of EEF2K was analyzed using GEPIA2 (<http://gepia2.cancer-pku.cn/>). Information on the protein subcellular localization of EEF2K was retrieved from The Human Protein Atlas (THPA) database (<https://www.proteinatlas.org/>). Interacting proteins with EEF2K were investigated using the STRING database (<https://cn.string-db.org/>).

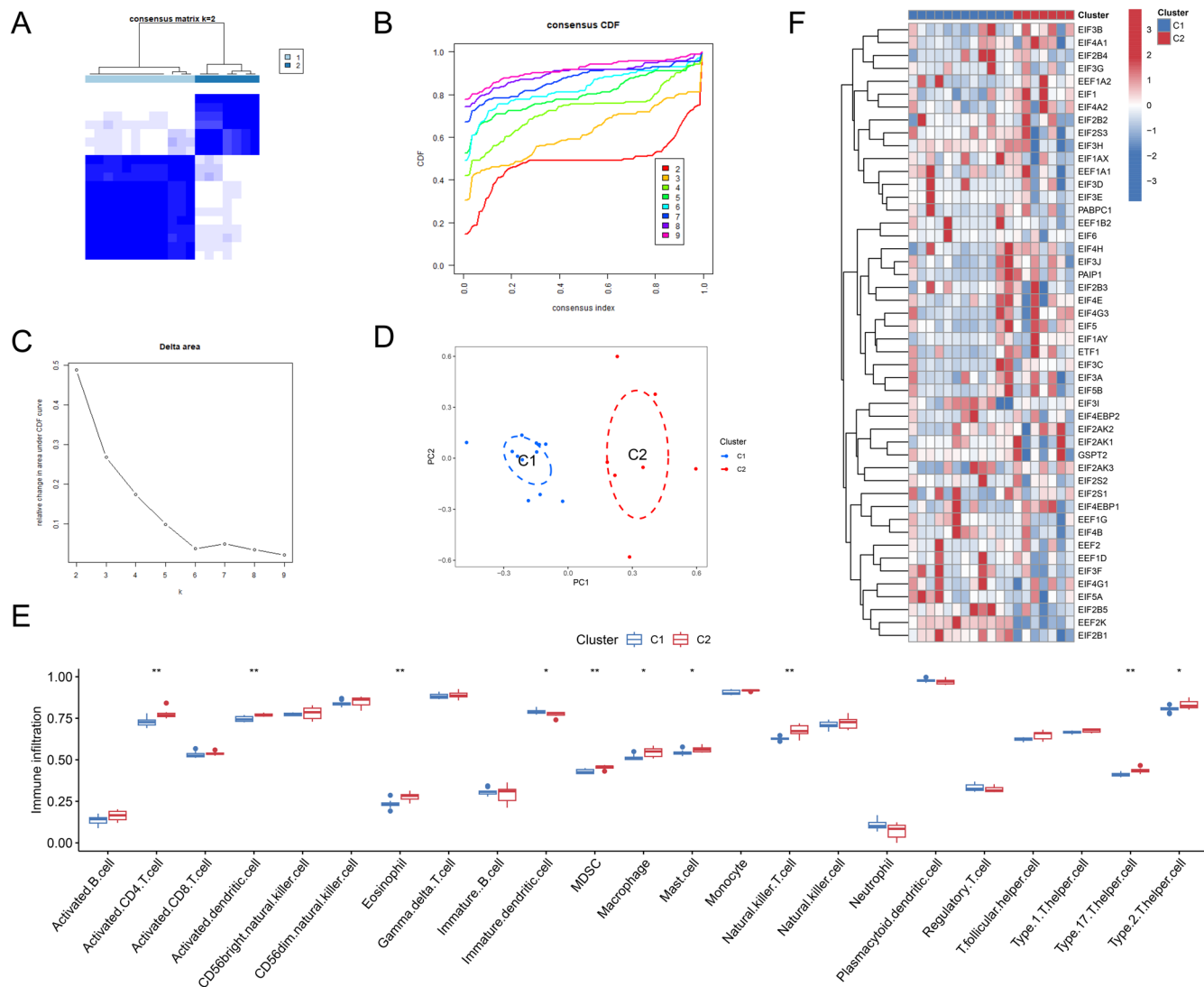


FIGURE 3 | First consensus cluster analysis: (A) Consensus matrices of the 9 significant TFGs for k = 2. (B) Consensus clustering CDF for k = 2–9. (C) Relative change in area under the CDF curve for k = 2–9. (D) PCA of the two clusters. (E) Boxplot of differences in the degree of immune cell infiltration. (F) Heatmap of TFGs for two clusters.

2.8 | Clinical Samples

Intervertebral disc tissues were obtained from the Second Affiliated Hospital of Nanchang University. Three cases of degenerative AF tissues were collected from patients who underwent discectomy for disc herniation, while three cases of normal AF tissues were obtained from patients who had surgery for trauma or scoliosis without IVDD. This study received approval from the Ethics Committee of the Second Affiliated Hospital of Nanchang University[I-2023(6)].

2.9 | Immunohistochemistry

The IVD tissue included 3 normal and 3 degenerative. *EEF2K* levels were assessed using immunohistochemistry (IHC). Rabbit anti-*EEF2K* antibody (Proteintech, 1:200, catalog number 13510-1-AP) was used for staining. NIKON Eclipse ci equipped with NIS_F_Ver43000_64bit_E software was used for observation and snapping.

3 | Results

3.1 | Data Processing

A total of thirty-five samples from three datasets—GSE27494, GSE17077, and GSE41833—were combined, including 16 normal samples and 19 degenerated samples. The samples were

normalized and merged to eliminate batch effects, ensuring that all three datasets were calibrated to the same level (Figure S1).

3.2 | Landscape of the TFGs

A total of 50 TFGs were analyzed. Initially, expression levels of these TFGs in normal versus degenerated IVD samples were compared, resulting in the identification of nine significantly differentially expressed TFGs: *EEF2K*, *EIF1*, *EIF2AK3*, *EIF2B1*, *EIF2B3*, *EIF2B5*, *EIF2S3*, *EIF3H*, and *GSPT2* (Figure 2A,B). *EIF1* and *EIF2AK3* were up-regulated in degenerated samples, whereas *EEF2K*, *EIF2B1*, *EIF2B3*, *EIF2B5*, *EIF2S3*, *EIF3H*, and *GSPT2* were downregulated. The chromosomal locations of these genes are depicted in Figure 2C. A heatmap illustrating correlations between gene expression levels across different samples is depicted in Figure 2D.

3.3 | Two Clusters Identified by Significant TFGs

Unsupervised clustering analysis of IVDD was conducted to examine expression patterns of TFGs based on the expression of nine TFGs. Two distinct clusters with different TFG patterns were identified (Figure 3A–C). Cluster 1 and Cluster 2 each comprised of seven samples. The ability of significant TFGs to differentiate between these patterns was further validated through PCA (Figure 3D). Additionally, immune

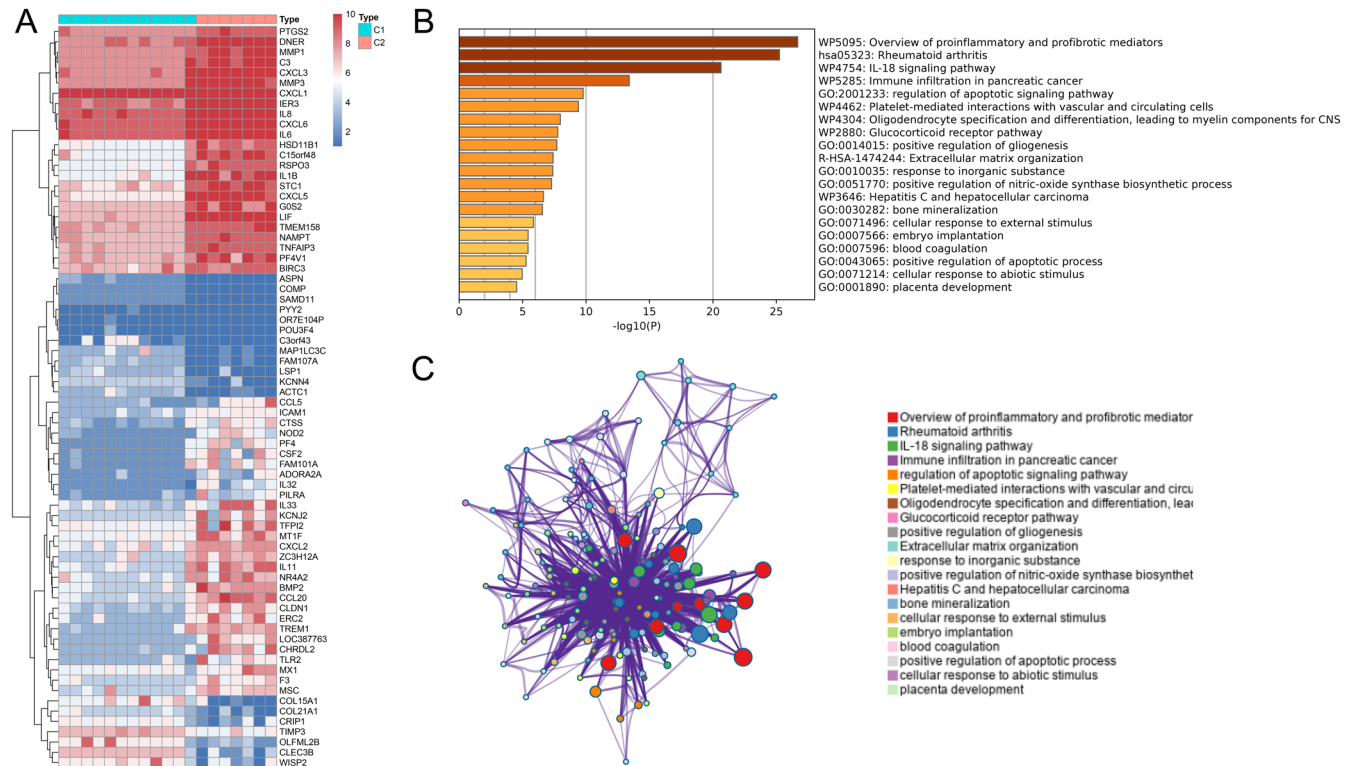


FIGURE 4 | Two-cluster enrichment analysis. (A) Heatmap displaying gene expression levels in the two clusters. (B) Bar chart for enrichment analysis. (C) Enhanced pathway regulatory network.

infiltration levels in the two clusters were assessed using ssGSEA. Cluster 2 demonstrated higher levels of immune infiltration compared to Cluster 1 (Figure 3E). Heatmaps illustrating TFG expression in the two clusters are depicted in Figure 3F.

3.4 | Enrichment Analysis of the Two Clusters

To interpret the intrinsic differences between the two clusters, several analyses were conducted. First, a heatmap was generated to display genes differing between the two clusters (Figure 4A). Notably, inflammation-related genes like IL6, IL8, and CXCL1, were highly expressed in Cluster 2. These genes were primarily enriched in the pathways “Overview of Proinflammatory and Profibrotic Mediators,” “IL-18 Signaling Pathway,” and “Immune Infiltration in Pancreatic Cancer” (Figure 4B). The pathway network analysis revealed close interactions among each other (Figure 4C).

3.5 | Identification of Two Gene Clusters

To gain insight into the significance of genes differentially expressed between the two clusters, a consensus clustering algorithm was used. This analysis identified two distinct gene clusters based on 72 differentially expressed genes (Figure 5A–C). PCA further demonstrated different distribution patterns between the two gene clusters (Figure 5D). Gene Cluster B exhibited notably higher levels of immune cell infiltration (Figure 5E). To elucidate the relationship between the clusters and gene clusters, a Sankey plot was constructed, revealing a significant level of correspondence (Figure 5F).

3.6 | Screening for Hub Genes by Machine Learning

Four models were developed using the training data to identify the characteristic TFGs for disease characterization and

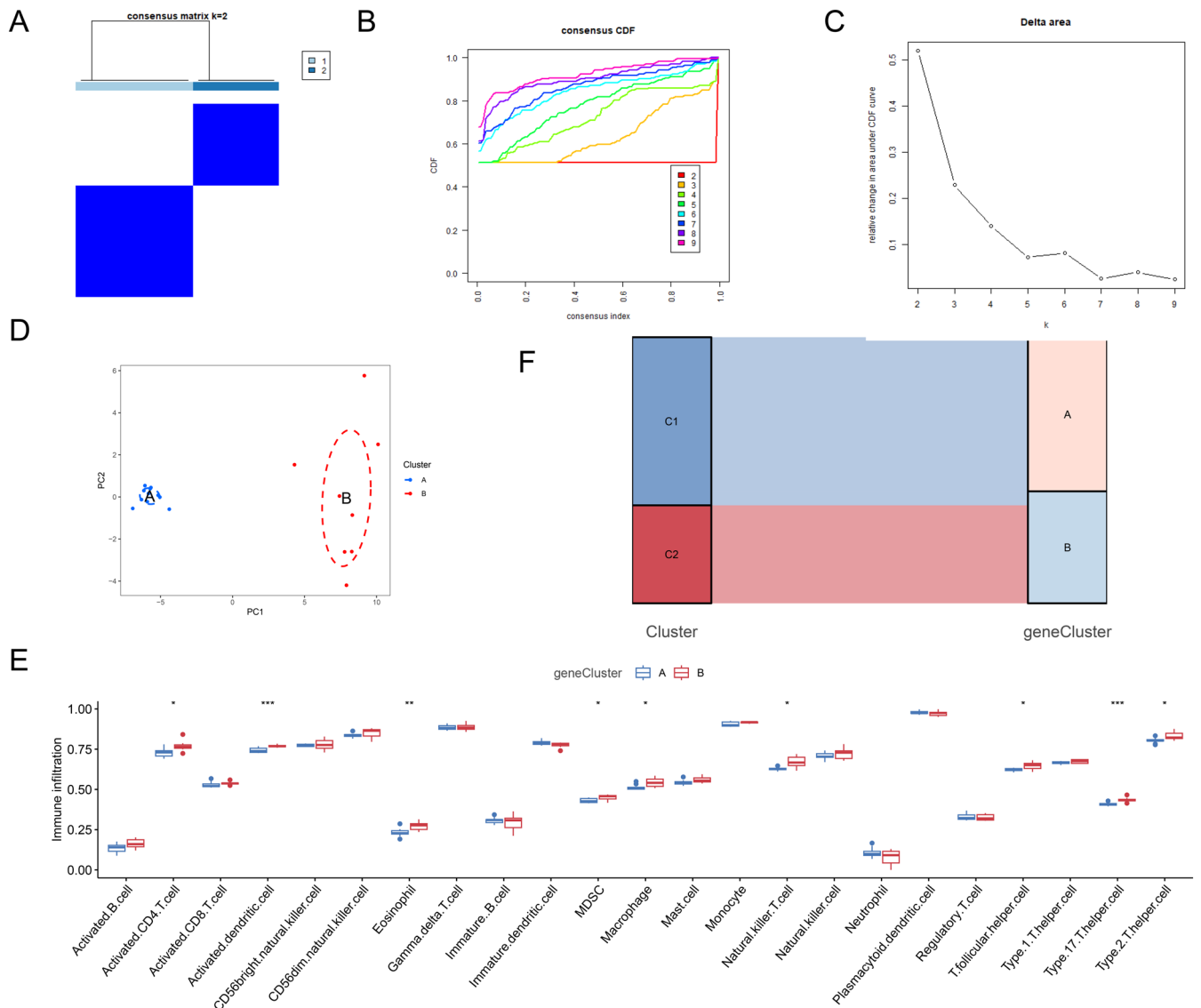


FIGURE 5 | Second consensus cluster analysis. (A) Consensus matrices of the differential gene between clusters at $k = 2$. (B) Consensus clustering CDF for $k = 2-9$. (C) Relative change in area under the CDF curve for $k = 2-9$. (D) Principal component analysis of the two gene clusters. (E) Boxplot depicting differences in immune cell infiltration. (F) The link between clusters and gene clusters.

IVDD incidence prediction. Residual box plots, inverse cumulative distributions of residuals, and ROC curves demonstrated that the SVM model exhibited superior prediction accuracy compared to the other models (Figure 6A–C). Consequently, the SVM model was selected. Box plots illustrated the importance of the five key variables considered in each of the four models (Figure 6D). A heatmap displayed the correlations between these five important TFGs and immune cells (Figure 6E).

3.7 | Construction of the TFGs-Based Predictive Model

Given that the SVM model was identified as optimal, the initial five genes (*GSPT2*, *EIF2B5*, *EEF2K*, *EIF2S3*, *EIF2B1*) from this model were selected for further analysis. A nomogram model was developed to estimate the probability of IVDD incidence based on these five key TF-related genes (Figure 7A). Calibration curves confirmed the accuracy of the TFG-based predictive model (Figure 7B). DCA curves proposed that the

decisions made by the TFG-based predictive model could be advantageous for patients diagnosed with IVDD (Figure 7C).

3.8 | Pan-Cancer Analysis of EEF2K

Given that *EEF2K* emerged as the most critical gene in the SVM model, a pan-cancer analysis was conducted. *EEF2K* was under expressed in tumors like BLCA, BRCA, COAD, and KICH, while it was overexpressed in tumors like CHOL, HNSC, KIRC, and KIRP, indicating its potential as a pan-cancer biomarker (Figure 8A). Survival analysis revealed that *EEF2K* expression was associated with poor survival outcomes in only a few malignancies (Figure 8B). Specifically, decreased *EEF2K* expression correlated with poor prognosis in HNSC and KIRC, whereas increased expression was linked to worse outcomes in THYM (Figure 8C). Additionally, immunofluorescence (IF) staining demonstrated that *EEF2K* was primarily localized in the nuclei of tumor cell lines (Figure 8D). Finally, a PPI network was constructed to illustrate the proteins closely associated with *EEF2K* (Figure 8E).

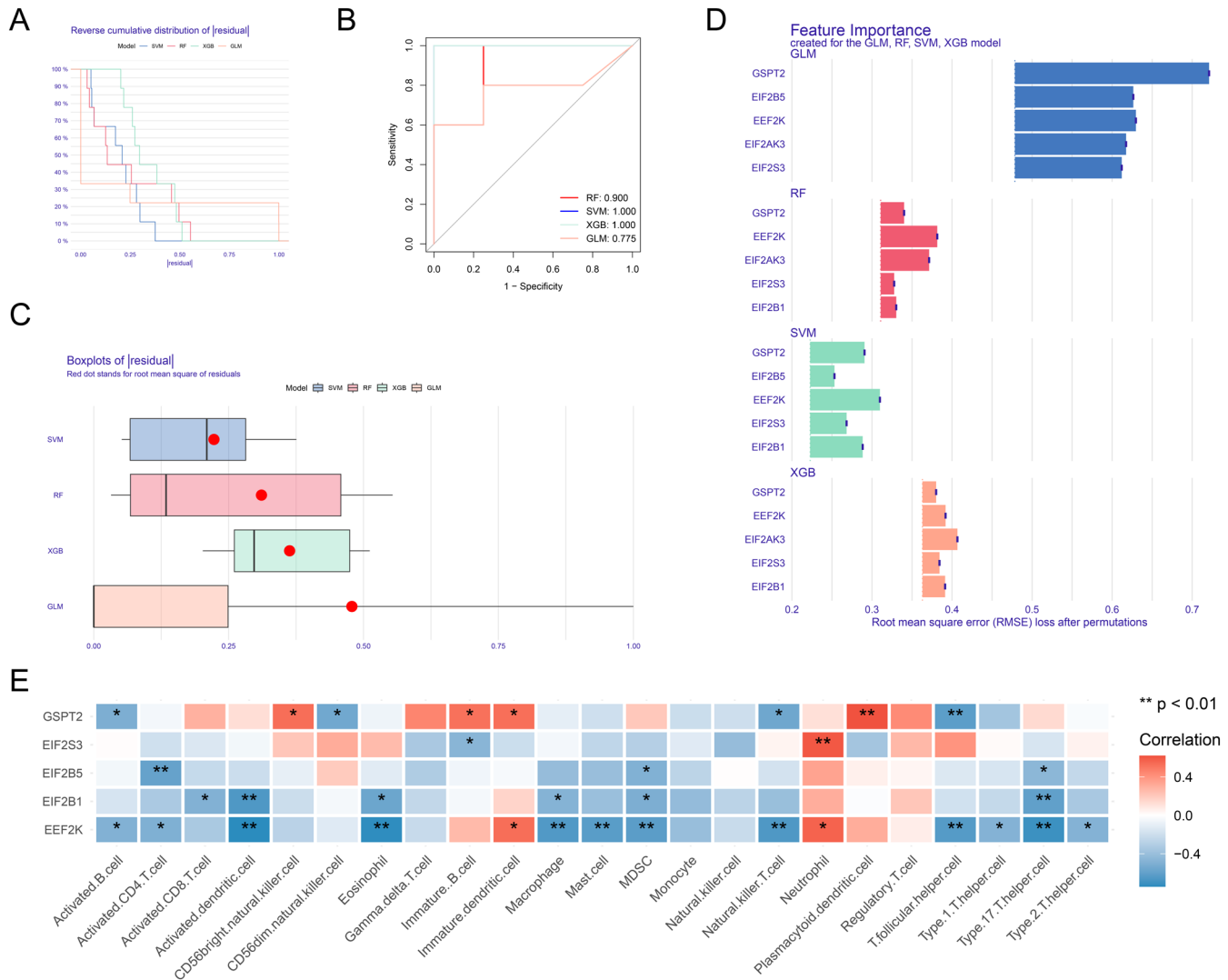


FIGURE 6 | Construction of the SVM model. (A) The cumulative residual distribution plot. (B) The nomogram's receiver operating characteristic curve. (C) A boxplot of the residuals. (D) The importance of variables. (E) Heatmap of the relationship between hub genes and various infiltrating immune cells.

3.9 | Low Expression of EEF2K in IVDD

EEF2K expression in IVDD was further validated. Box plots from the integrated dataset revealed low expression of EEF2K in degenerative AF tissues (Figure 9A). EEF2K demonstrated high diagnostic potential as a marker (Figure 9B). To corroborate these findings, the GSE70362 dataset was used as a validation set, which confirmed the diagnostic value and differential expression of EEF2K (Figure 9C,D). Additionally, IHC staining further validated the low expression of EEF2K in AF tissue from degenerated discs (Figure 9E).

3.10 | Potential EEF2K Mechanisms

To examine the underlying EEF2K mechanisms, GSEA was conducted. In the GO analysis, EEF2K was associated with processes like “granulocyte chemotaxis,” “granulocyte migration,” “leukocyte chemotaxis,” “myeloid leukocyte migration,” “neutrophil chemotaxis,” and “neutrophil migration” (Figure 10A). The KEGG analysis revealed that EEF2K was involved in pathways including “chemokine signaling pathway,”

“cytokine-cytokine receptor interaction,” “JAK/STAT signaling pathway,” “Nod-like receptor signaling pathway,” and “Toll-like receptor signaling pathway” (Figure 10B).

4 | Discussion

LBP is a major global cause of disability, significantly contributing to social and economic burdens [13]. In the United States, LBP ranks as the second most common reason for physician visits, the fifth most common cause of hospitalization, and the third most frequent reason for surgical intervention [14, 15]. IVDD is widely acknowledged as the primary cause of LBP [16]. Surgical intervention for IVDD typically involves the removal of degenerated or prominent tissue [17, 18]. However, such procedures may lead to adjacent disc degeneration or other complications [19]. Therefore, identifying IVDD heterogeneity, elucidating underlying mechanisms, and identifying key genes are key areas of focus. The IVD comprises of the inner NP and the surrounding AF. The AF consists of highly organized collagen fibers arranged in a fibrous laminar structure, with 15–25 layers of collagen types I (Col-I) and II (Col-II). The AF is essential for

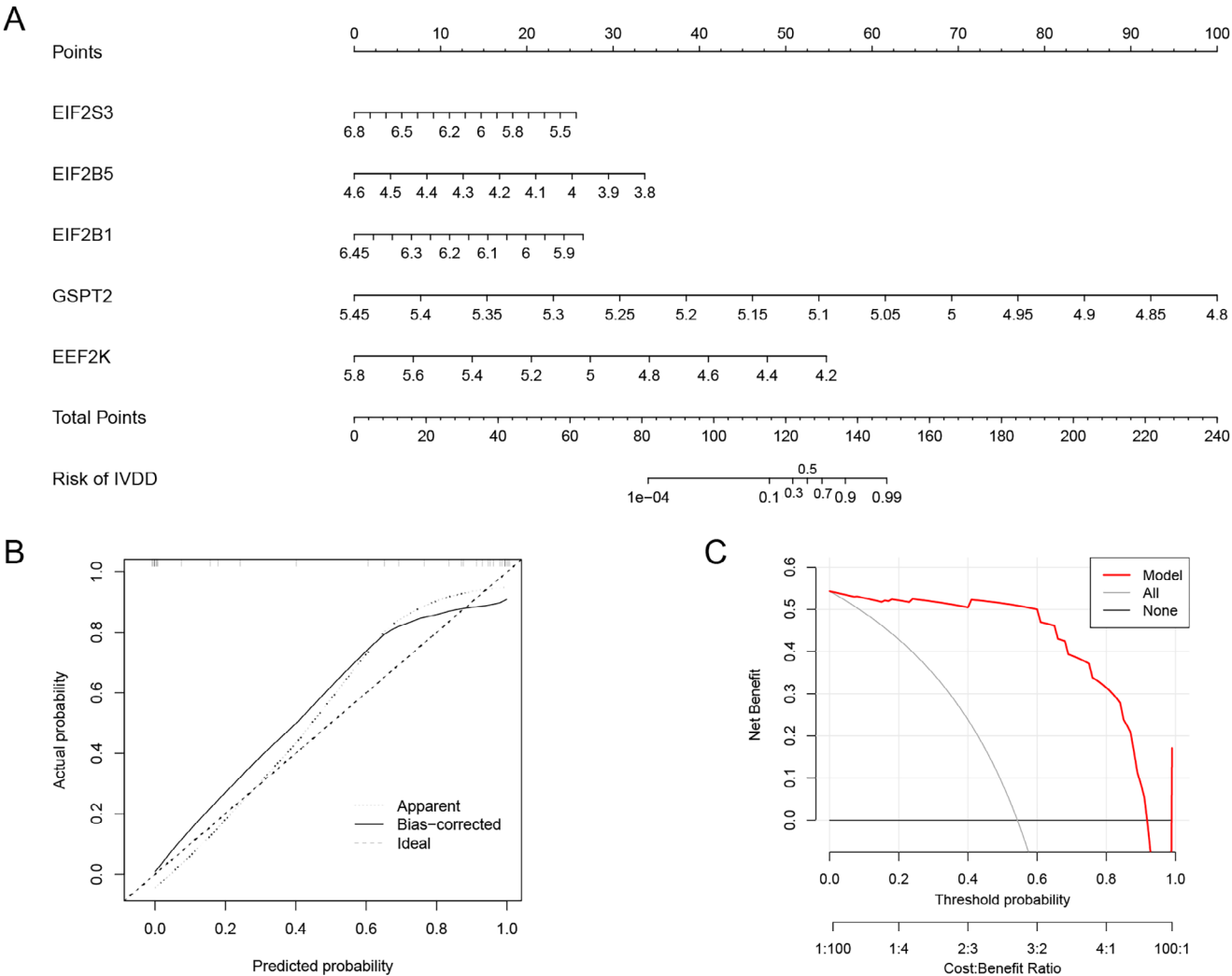


FIGURE 7 | Developing and validating a nomogram model for IVDD diagnosis. (A) A nomogram of diagnostic biomarkers used to predict IVDD. (B) The calibration curve is used to assess the nomogram model’s predictive power. (C) The DCA curve is used to assess the clinical application value of the nomogram model.

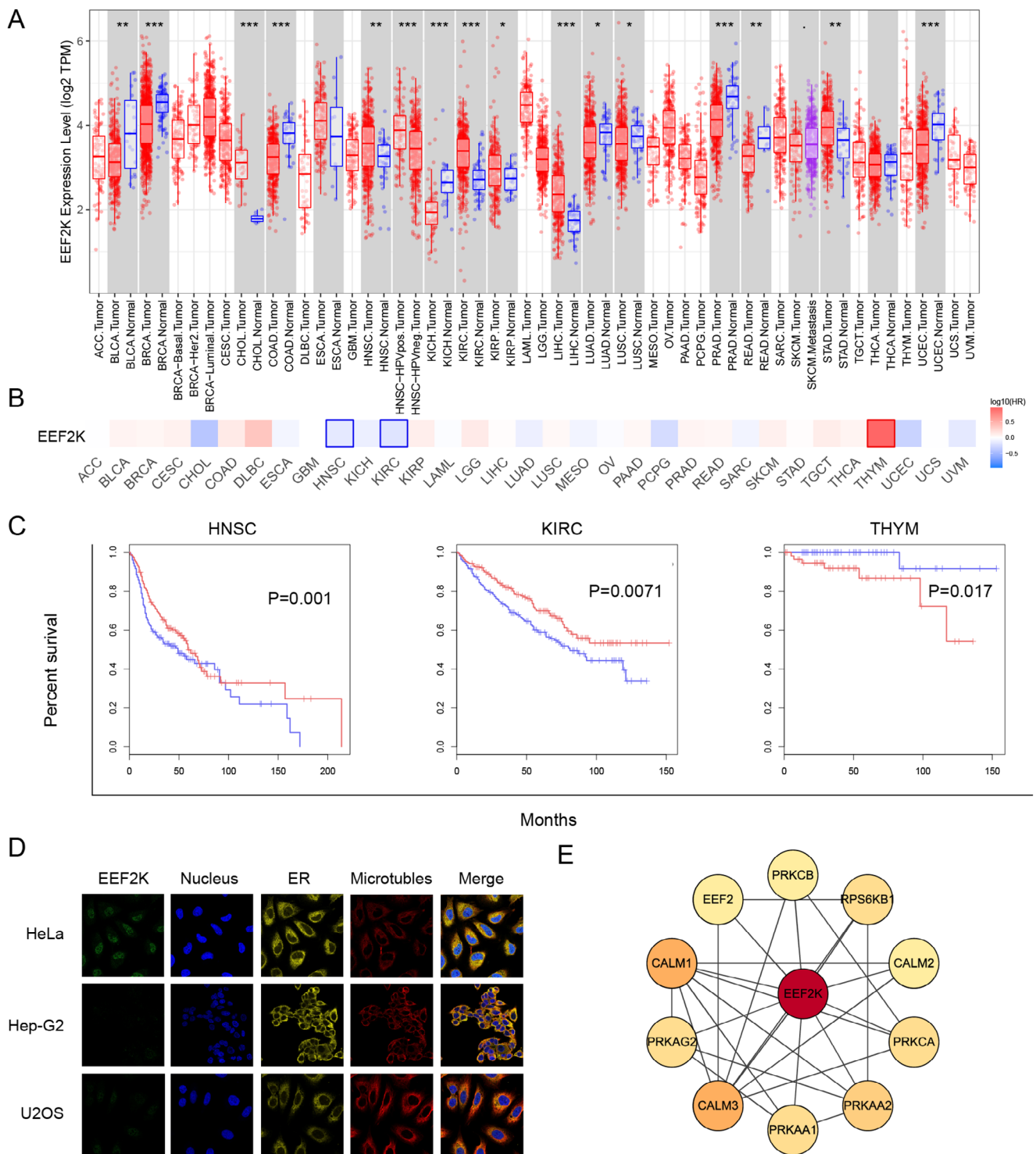


FIGURE 8 | EEF2K has been studied across multiple cancers. (A) A pan-cancer study of EEF2K expression using the TIMER. (B) EEF2K survival map in pan-cancer. (C) Kaplan-Meier survival curves for total survival. (D) Immunofluorescence images indicate EEF2K protein expression in the nucleus, endoplasmic reticulum (ER), and microtubules of HeLa, Hep-G2, and U2OS cells. (E) The PPI network of EEF2K.

generating significant circumferential stresses and withstanding substantial tensile and compressive forces. It plays a crucial role in maintaining the biomechanical integrity of the IVD [20]. Consequently, research on the AF is a focal point of our study.

Numerous studies have used microarray technology to examine indicators and key pathways associated with IVDD. Smolders et al. reported that the Wnt signaling pathway is downregulated

in early IVDD [21]. Gruber et al. analyzed gene expression patterns related to pain, nerve function, and neurotrophic factors in human IVD [22]. Additionally, Gruber and Wan et al. identified several aberrantly expressed lncRNAs [23, 24]. High-throughput microarray analyses have significantly advanced the understanding of the potential pathogenesis of IVDD. The global regulation of mRNA translation is critical for controlling cellular activities. Aberrant levels of mRNA translation-associated

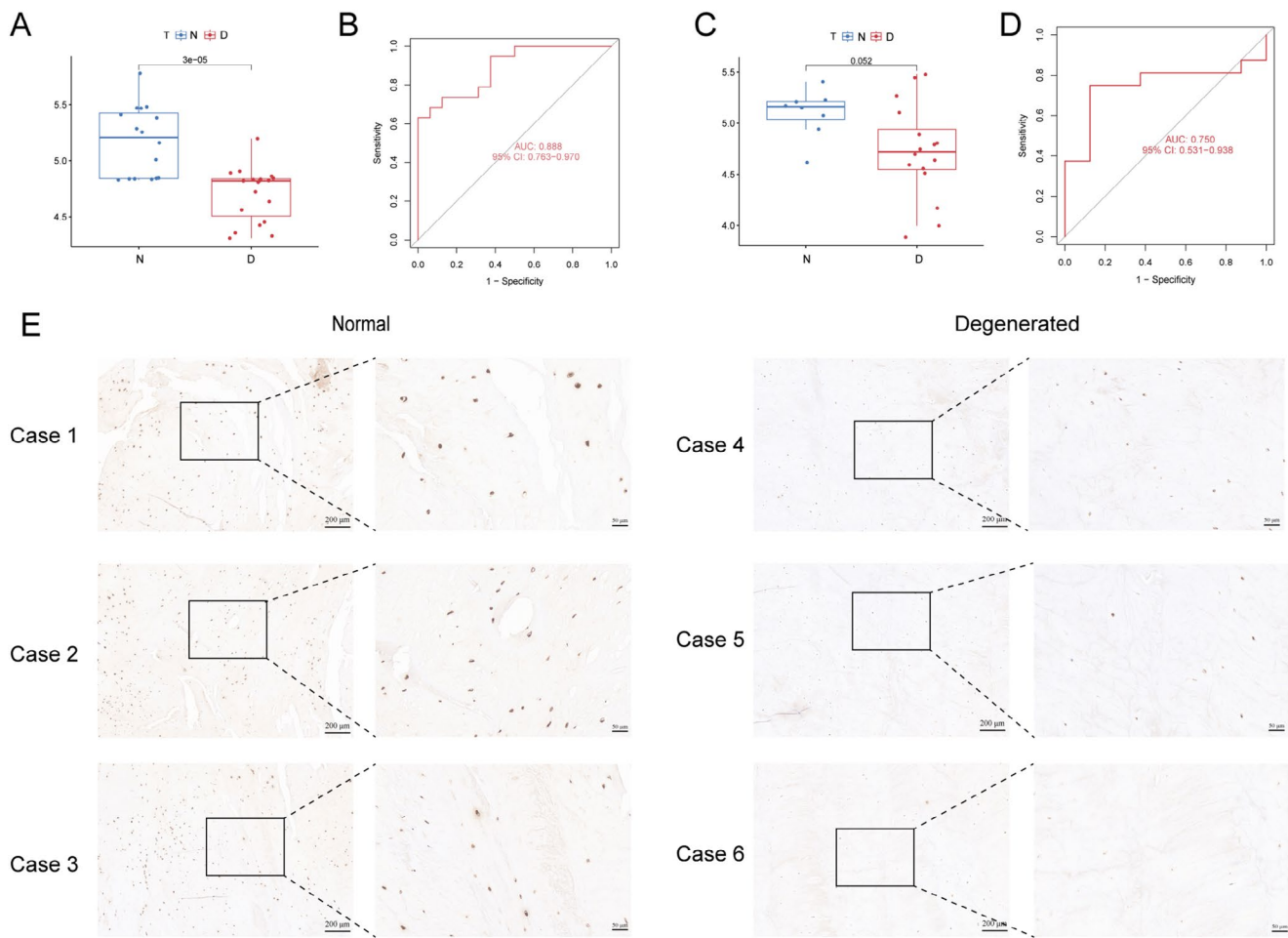


FIGURE 9 | Expression levels of EEF2K. (A, C) EEF2K expression was lower using the merged datasets (GSE41883, GSE27494, and GSE17077) and the external validation set (GSE70362). (B, D) ROC analysis of EEF2K. (E) Immunohistochemical staining reveals low levels of IVDD.

factors may contribute to disease development. Despite this, the specific role of TF in IVDD remains unclear, warranting further investigation.

We identified nine significant genes from the 50 TFGs and used these to subtype the IVDD samples. Various analyses, including immune infiltration and PCA, revealed that the results were highly consistent across the subtyped IVDD samples. Subsequently, a nomogram based on an SVM model was developed to estimate the likelihood of IVDD occurrence. The low expression of EEF2K was validated using external datasets and IHC, while its significance in pan-cancer contexts was examined.

Protein synthesis regulation is critical for eukaryotic organisms, with EEF2K serving as a key regulator that inhibits protein translation to conserve biological energy [25, 26]. Aberrant EEF2K expression has been linked to the prognosis of various cancers, including melanoma, pancreatic cancer, and lung cancer [27–29]. Additionally, EEF2K plays a vital role in regulating the metabolism of certain immune cells. Chen et al. demonstrated that EEF2K enhances PD-L1 stability and expression by inactivating GSK3 β , thereby helping cancer cells evade immune surveillance [29]. In this study, EEF2K was downregulated in IVDD, and single-gene GSEA indicated that inflammatory pathways might underlie this observation.

IVD is traditionally considered an organ with a privileged immune environment, exhibiting a minimal presence of immune cells [30]. However, damage to the AF or cartilaginous endplate (CEP) can lead to angiogenesis and subsequent immune cell infiltration into the disc. This infiltration exacerbates the inflammatory environment within the IVD, resulting in increased expression of cytokines and chemokines [31]. This process accelerates the breakdown of the extracellular matrix (ECM) [32]. Cytokines and chemokines have a direct impact on the NP, AF, and CEP cells, and may also extend beyond the IVD, potentially leading to localized nerve root sensitization or enhanced migration of cells to the IVD [33–36]. Lee et al. [37] found significant macrophage infiltration in mouse degenerated discs, which is consistent with the findings of Silva et al. [38] that macrophages may induce disc degeneration by regulating the expression of proteoglycan and collagen-II-related genes and interfering with the synthesis of extracellular matrix mediated by interleukin 1 β . Wang et al. [39] speculated that a special type of immune microenvironment is generated in the pathological process of disc degeneration, in which macrophages and regulatory T cells (Tregs) are recruited, and these immune cells regulate ID1, PTPRK, and RAP2C genes through signaling pathways such as transforming growth factor β and MAPK, which leads to pathological changes in the disc. Ling et al. [40] performed scRNA-seq analysis of three

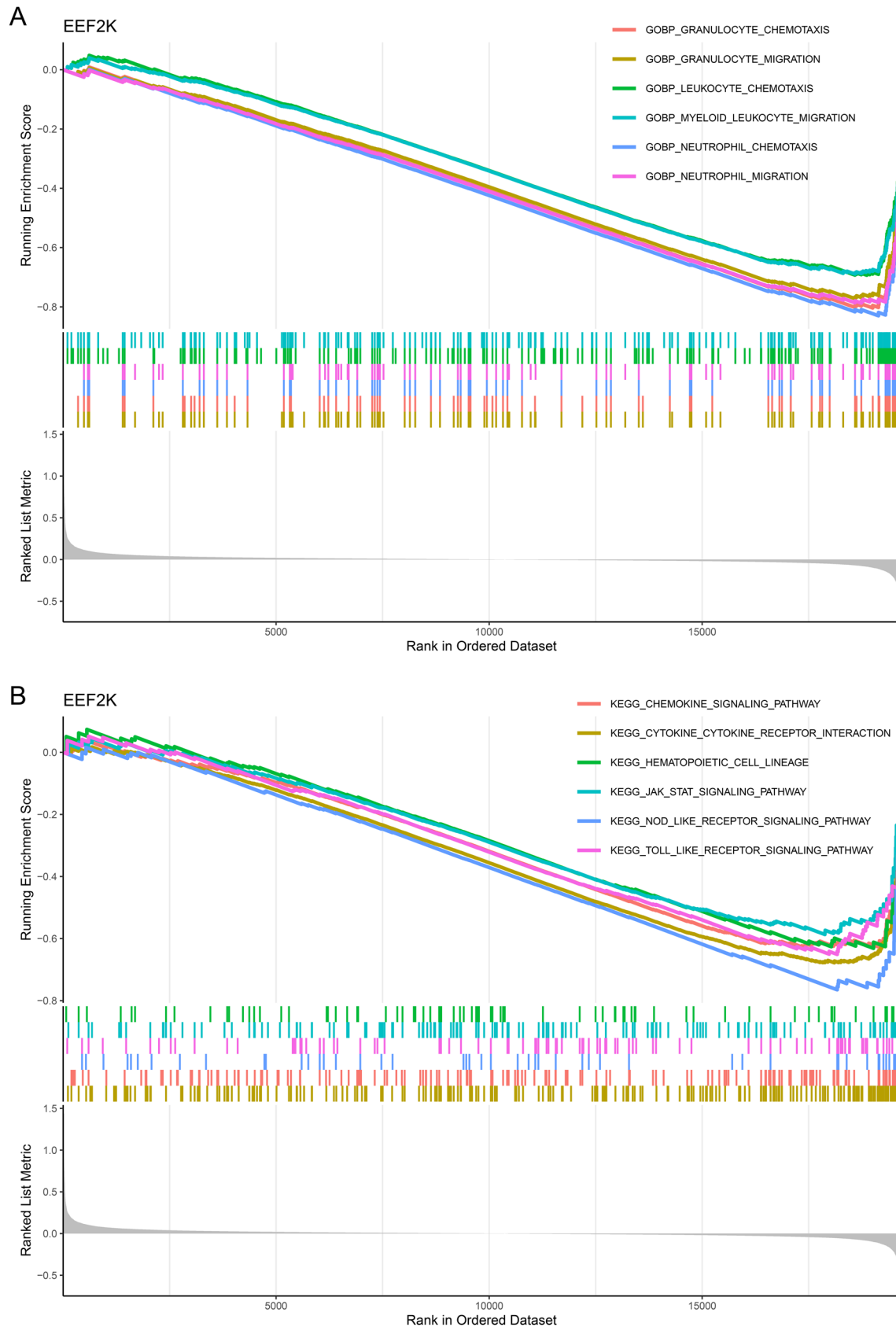


FIGURE 10 | Enrichment analysis results for the GSEA gene set. (A) Go terms. (B) KEGG pathway.

human NP tissues with Pfirrmann grades II, III, and IV and identified immune cells including macrophages, T cells, myeloid progenitor cells, and neutrophils; functional analysis showed that most of these immune cells were involved in neutrophil activation, neutrophil degranulation, and related pathways such as apoptotic signaling and apoptotic signaling. Trajectory analysis showed that ApoE induced activation of M1 macrophages and a decrease in the proportion of M2 macrophages during disc degeneration, suggesting that dynamic polarization of M1 and M2 subtypes of macrophages may play an important role in amplifying the inflammatory cascade; cell communication analysis showed that nuclear factor κ B-mediated macrophage polarization may induce an inflammatory response through the MIF signaling pathway. Significant differences in immune cell infiltration were observed among clusters in our study. Additionally, single-gene GSEA for EEF2K proposes that immune mechanisms may be involved. These findings imply that TFGs likely play a role in regulating immune infiltration and, consequently, in IVDD progression.

To summarize, this study introduces a new genetic subtype based on TFGs and develops a predictive model. Nevertheless, several limitations must be acknowledged. First, despite the integration of multiple microarray datasets, the sample size remains relatively small. Second, the clinical data available were insufficient, and more comprehensive clinical information is needed to fully assess the association between subtypes and clinical outcomes. Finally, further research is necessary to clarify the molecular pathways associated with these findings. These aspects will be addressed in future studies.

5 | Conclusion

TFGs are valuable for distinguishing between different IVDD clusters. The predictive model developed demonstrates strong performance in forecasting IVDD. A thorough analysis of these clusters can contribute to a deeper understanding of the molecular mechanisms of IVDD.

Author Contributions

Conception and design of the research: Sikuan Zheng, Dingwen He. Acquisition of data: Xiaokun Zhao, Hui Wu, Xuhui Cuan. Analysis and interpretation of the data: Sikuan Zheng, Xiaokun Zhao. Statistical analysis: Sikuan Zheng, Hui Wu, Xuhui Cuan. Writing of the manuscript: Sikuan Zheng, Xigao Cheng. Critical revision of the manuscript for intellectual content: Sikuan Zheng, Xigao Cheng, Dingwen He. All authors read and approved the final draft.

Acknowledgments

We would like to acknowledge the hard and dedicated work of all the staff who implemented the intervention and evaluation components of the study.

Ethics Statement

This study was conducted with approval from the Ethics Committee of the Second Affiliated Hospital of Nanchang University[1-2023(6)]. This study was conducted in accordance with the declaration of Helsinki. Written informed consent was obtained from all participants.

Consent

The authors have nothing to report.

Conflicts of Interest

The authors declare no conflicts of interest.

Data Availability Statement

The datasets supporting the conclusions of this article are available in the Gene Expression Omnibus (<https://www.ncbi.nlm.nih.gov/geo/>).

References

1. R. A. Deyo, S. F. Dworkin, D. Amtmann, et al., "Report of the NIH Task Force on Research Standards for Chronic Low Back Pain," *Spine Journal* 14, no. 8 (2014): 1375–1391.
2. S. Sharifi, S. K. Bulstra, D. W. Grijpma, and R. Kuijer, "Treatment of the Degenerated Intervertebral Disc; Closure, Repair and Regeneration of the Annulus Fibrosus," *Journal of Tissue Engineering and Regenerative Medicine* 9, no. 10 (2015): 1120–1132, <https://doi.org/10.1002/term.1866>.
3. Y. Huang, X. Qiu, J. Liu, et al., "Identification of Biomarkers, Pathways, Immune Properties of Mitophagy Genes, and Prediction Models for Intervertebral Disc Degeneration," *Journal of Inflammation Research* 17 (2024): 2959–2975, <https://doi.org/10.2147/JIR.S461668>.
4. C. Song, Y. Zhou, K. Cheng, et al., "Cellular Senescence - Molecular Mechanisms of Intervertebral Disc Degeneration From an Immune Perspective," *Biomedicine & Pharmacotherapy* 162 (2023): 114711, <https://doi.org/10.1016/J.BIOPHA.2023.114711>.
5. J. Kawamoto, T. Kurihara, M. Kitagawa, I. Kato, and N. Esaki, "Proteomic Studies of an Antarctic Cold-Adapted Bacterium, *Shewanella livingstonensis* Ac10, for Global Identification of Cold-Inducible Proteins," *Extremophiles: Life Under Extreme Conditions* 11, no. 6 (2007): 819–826.
6. J. Knight, G. Garland, T. Pöyry, et al., "Control of Translation Elongation in Health and Disease," *Disease Models & Mechanisms* 13, no. 3 (2020): DMM043208, <https://doi.org/10.1242/DMM.043208>.
7. V. Lefebvre, M. Angelozzi, and A. Haseeb, "SOX9 in Cartilage Development and Disease," *Current Opinion in Cell Biology* 61 (2019): 39–47, <https://doi.org/10.1016/J.CEB.2019.07.008>.
8. G. Hu, Y. Yu, Y. Tang, C. Wu, F. Long, and C. Karner, "The Amino Acid Sensor EIF2AK4/GCN2 Is Required for Proliferation of Osteoblast Progenitors in Mice," *Journal of Bone and Mineral Research* 35, no. 10 (2020): 2004–2014, <https://doi.org/10.1002/JBMR.4091>.
9. S. J. Watkins and C. J. Norbury, "Translation Initiation and Its De-regulation During Tumorigenesis," *British Journal of Cancer* 86, no. 7 (2002): 1023–1027.
10. M. Eyries, D. Montani, B. Girerd, et al., "EIF2AK4 Mutations Cause Pulmonary Veno-Occlusive Disease, a Recessive Form of Pulmonary Hypertension," *Nature Genetics* 46, no. 1 (2014): 65–69.
11. W. N. Xu, C. Liu, H. L. Zheng, et al., "Sesn2 Serves as a Regulator Between Mitochondrial Unfolded Protein Response and Mitophagy in Intervertebral Disc Degeneration," *International Journal of Biological Sciences* 19, no. 2 (2023): 571–592, <https://doi.org/10.7150/ijbs.70211>.
12. W. Lin, "Impaired eIF2B Activity in Ligodendrocytes Contributes to VWMD Pathogenesis," *Neural Regeneration Research* 10, no. 2 (2015): 195–197.
13. G. Chu, C. Shi, H. Wang, W. Zhang, H. Yang, and B. Li, "Strategies for Annulus Fibrosus Regeneration: From Biological Therapies to Tissue Engineering," *Frontiers in Bioengineering and Biotechnology* 6 (2018): 90.

14. V. M. Taylor, R. A. Deyo, D. C. Cherkin, and W. Kreuter, "Low Back Pain Hospitalization. Recent United States Trends and Regional Variations," *Spine* 19, no. 11 (1994): 1207–1212.
15. L. G. Hart, R. A. Deyo, and D. C. Cherkin, "Physician Office Visits for Low Back Pain. Frequency, Clinical Evaluation, and Treatment Patterns From a U.S. National Survey," *Spine* 20, no. 1 (1995): 11–19.
16. N. Boos, N. Semmer, A. Elfering, et al., "Natural History of Individuals With Asymptomatic Disc Abnormalities in Magnetic Resonance Imaging: Predictors of Low Back Pain-Related Medical Consultation and Work Incapacity," *Spine* 25, no. 12 (2000): 1484–1492.
17. Z. Kazezian, R. Gawri, L. Haglund, et al., "Gene Expression Profiling Identifies Interferon Signalling Molecules and IGFBP3 in Human Degenerative Annulus Fibrosus," *Scientific Reports* 5 (2015): 15662.
18. J. N. Gibson and G. Waddell, "Surgical Interventions for Lumbar Disc Prolapse: Updated Cochrane Review," *Spine* 32, no. 16 (2007): 1735–1747.
19. H. Frei, T. R. Oxland, G. C. Rathonyi, and L. P. Nolte, "The Effect of Nucleotomy on Lumbar Spine Mechanics in Compression and Shear Loading," *Spine* 26, no. 19 (2001): 2080–2089.
20. L. Zhao, B. Tian, Q. Xu, C. Zhang, L. Zhang, and H. Fang, "Extensive Mechanical Tension Promotes Annulus Fibrosus Cell Senescence Through Suppressing Cellular Autophagy," *Bioscience Reports* 39, no. 4 (2019): 0163.
21. L. A. Smolders, B. P. Meij, D. Onis, et al., "Gene Expression Profiling of Early Intervertebral Disc Degeneration Reveals a Down-Regulation of Canonical Wnt Signaling and Caveolin-1 Expression: Implications for Development of Regenerative Strategies," *Arthritis Research & Therapy* 15, no. 1 (2013): R23, <https://doi.org/10.1186/ar4157>.
22. H. E. Gruber, G. L. Hoelscher, J. A. Ingram, and E. N. Hanley, Jr., "Genome-Wide Analysis of Pain-, Nerve- and Neurotrophin -Related Gene Expression in the Degenerating Human Annulus," *Molecular Pain* 8 (2012): 63.
23. H. E. Gruber, J. A. Watts, G. L. Hoelscher, et al., "Mitochondrial Gene Expression in the Human Annulus: In Vivo Data From Annulus Cells and Selectively Harvested Senescent Annulus Cells," *Spine Journal* 11, no. 8 (2011): 782–791.
24. Z. Y. Wan, F. Song, Z. Sun, et al., "Aberrantly Expressed Long Non-coding RNAs in Human Intervertebral Disc Degeneration: A Microarray Related Study," *Arthritis Research & Therapy* 16, no. 5 (2014): 465.
25. A. G. Ryazanov, M. D. Ward, C. E. Mendola, et al., "Identification of a New Class of Protein Kinases Represented by Eukaryotic Elongation Factor-2 Kinase," *Proceedings of the National Academy of Sciences of the United States of America* 94, no. 10 (1997): 4884–4889.
26. M. Yang and G. H. Xu, "Isobaric Tag for Relative and Absolute Quantitation-Based Proteomics for Investigating the Effect of Guasha on Lumbar Disc Herniation in Rats," *World Journal of Traditional Chinese Medicine* 9 (2023): 160–166.
27. M. Xiao, J. Xie, Y. Wu, et al., "The eEF2 Kinase-Induced STAT3 Inactivation Inhibits Lung Cancer Cell Proliferation by Phosphorylation of PKM2," *Cell Communication and Signaling* 18, no. 1 (2020): 25.
28. D. Karakas and B. Ozpolat, "Eukaryotic Elongation Factor-2 Kinase (EEF2K) Signaling in Tumor and Microenvironment as a Novel Molecular Target," *Journal of Molecular Medicine (Berlin, Germany)* 98, no. 6 (2020): 775–787.
29. X. Chen, K. Wang, S. Jiang, et al., "EEF2K Promotes PD-L1 Stabilization Through Inactivating GSK3 β in Melanoma," *Journal for Immunotherapy of Cancer* 10, no. 3 (2022): e004026.
30. Z. Sun, B. Liu, and Z. J. Luo, "The Immune Privilege of the Intervertebral Disc: Implications for Intervertebral Disc Degeneration Treatment," *International Journal of Medical Sciences* 17, no. 5 (2020): 685–692.
31. K. L. Phillips, K. Cullen, N. Chiverton, et al., "Potential Roles of Cytokines and Chemokines in Human Intervertebral Disc Degeneration: Interleukin-1 Is a Master Regulator of Catabolic Processes," *Osteoarthritis and Cartilage* 23, no. 7 (2015): 1165–1177.
32. M. V. Risbud and I. M. Shapiro, "Role of Cytokines in Intervertebral Disc Degeneration: Pain and Disc Content," *Nature Reviews Rheumatology* 10, no. 1 (2014): 44–56.
33. C. L. Le Maitre, J. A. Hoyland, and A. J. Freemont, "Catabolic Cytokine Expression in Degenerate and Herniated Human Intervertebral Discs: IL-1 β and TNF α Expression Profile," *Arthritis Research & Therapy* 9, no. 4 (2007): R77.
34. C. L. Le Maitre, A. J. Freemont, and J. A. Hoyland, "The Role of Interleukin-1 in the Pathogenesis of Human Intervertebral Disc Degeneration," *Arthritis Research & Therapy* 7, no. 4 (2005): R732–R745.
35. G. Pattappa, M. Peroglio, D. Sakai, et al., "CCL5/RANTES Is a Key Chemoattractant Released by Degenerative Intervertebral Discs in Organ Culture," *European Cells & Materials* 27 (2014): 124–136, 136.
36. L. Leung and C. M. Cahill, "TNF-Alpha and Neuropathic Pain—a Review," *Journal of Neuroinflammation* 7 (2010): 27.
37. S. Lee, M. Millecamps, D. Z. Foster, and L. S. Stone, "Long-Term Histological Analysis of Innervation and Macrophage Infiltration in a Mouse Model of Intervertebral Disc Injury-Induced Low Back Pain," *Journal of Orthopaedic Research* 38, no. 6 (2020): 1238–1247, <https://doi.org/10.1002/jor.24560>.
38. A. J. Silva, J. R. Ferreira, C. Cunha, et al., "Macrophages Down-Regulate Gene Expression of Intervertebral Disc Degenerative Markers Under a pro-Inflammatory Microenvironment," *Frontiers in Immunology* 10 (2019): 1508, <https://doi.org/10.3389/fimmu.2019.01508>.
39. L. Wang, T. He, J. Liu, et al., "Revealing the Immune Infiltration Landscape and Identifying Diagnostic Biomarkers for Lumbar Disc Herniation," *Frontiers in Immunology* 12 (2021): 666355, <https://doi.org/10.3389/fimmu.2021.666355>.
40. Z. Ling, Y. Liu, Z. Wang, et al., "Single-Cell RNA-Seq Analysis Reveals Macrophage Involved in the Progression of Human Intervertebral Disc Degeneration," *Frontiers in Cell and Development Biology* 9 (2022): 833420, <https://doi.org/10.3389/fcell.2021.833420>.

Supporting Information

Additional supporting information can be found online in the Supporting Information section.